# Vibrational Energy Distributions of $NH_2(\tilde{X}^2B_1)$ Fragments Generated in the Photolysis of $NH_3$ at 193 nm: Application of Kinetic Analysis on Vibrational Cascade

**Katsuyoshi Yamasaki,* Akihiro Watanabe,† Teruaki Kakuda, Akira Itakura, Hirofumi Fukushima, Masami Endo, Chiho Maruyama, and Ikuo Tokue**

*Department of Chemistry, Niigata University, Ikarashi, Niigata 950-2181, Japan*

*Received: April 11, 2002; In Final Form: June 10, 2002*

Nascent vibrational distributions of $NH_2(\tilde{X}^2B_1, v_2'' = 0-4)$ generated in the 193 nm photolysis of $NH_3$ at $298 \pm 1$ K have been determined by simple kinetic analysis. The vibrational levels of $NH_2(\tilde{X}^2B_1)$ were detected by laser-induced fluorescence (LIF) excited via the $\tilde{A}^2A_1-\tilde{X}^2B_1$ system, and time-resolved concentration profiles were recorded. Rate constants for intramode relaxation of $\nu_2$ vibration ($v_2'' \rightarrow v_2''-1$) by collisions of He have been determined to be $(4.2 \pm 1.0) \times 10^{-14}$, $(7.5 \pm 0.5) \times 10^{-14}$, $(1.6 \pm 0.1) \times 10^{-13}$, $(3.0 \pm 0.1) \times 10^{-13}$ in units of cm$^3$ molecule$^{-1}$ s$^{-1}$ for $v_2'' = 1$, 2, 3, and 4, respectively. The quoted errors are $2\sigma$. Rate constants for intermode coupling between $v_1'' = 1$ and $v_2'' = 2$ by He have also been determined to be $(4.7 \pm 1.6) \times 10^{-12}$ ($v_1'' = 1 \rightarrow v_2'' = 2$) and $(1.3 \pm 0.4) \times 10^{-12}$ cm$^3$ molecule$^{-1}$ s$^{-1}$ ($v_1'' = 1 \leftarrow v_2'' = 2$). Relative detectivities of the levels $v_2'' = 1-4$ were obtained by the kinetic analysis, and vibrational distributions immediately after the photolysis have been given to be $2.2 \pm 0.7/1.0/ < 1.3/0.66 \pm 0.3/ < 3.0$ for $v_2'' = 0/1/2/3/4$ (normalized by the population of $v_2'' = 1$). To the best of our knowledge, this is the first quantitative report on the initial vibrational populations of $NH_2$ generated in the photolysis at 193 nm.

## Introduction

The photolysis of ammonia ($NH_3$) has attracted the attention of many researchers, and there have been many experimental studies on the energy disposition and stereodynamics.[1−35] The ground electronic state $\tilde{X}^1A_1$ of $NH_3$ is nonplanar ($C_{3v}$ point group), and the first excited state $\tilde{A}^1A_2''$ is planar ($D_{3h}$). A photoabsorption spectrum via the $\tilde{A}^1A_2''-\tilde{X}^1A_1$ transition, therefore, shows a clear progression of out-of-plane ($\nu_2$) vibration.[36] The potential curve of the $\tilde{A}$ state has a shallow minimum along an N−H bond and correlates to $NH_2 + H$ beyond a barrier whose height is 2075 cm$^{-1}$.[31] The energies of the lowest two vibrational levels $v_2' = 0$ and 1 of $\tilde{A}$ state are lower than the barrier; however, these levels predissociate to $NH_2(\tilde{X}^2B_1) + H(^2S)$ due to tunneling effect.[19] Another product channel $NH_2(\tilde{A}^2A_1) + H(^2S)$ is energetically accessible when the vibrational levels $v_2' \geq 3$ of $NH_3(\tilde{A})$ are excited.[22] Branching ratios between the two states of $NH_2$, $\tilde{X}^2B_1$ and $\tilde{A}^2A_1$, are governed by the molecular symmetry of dissociating $NH_3$. When $NH_3$ is planar during dissociation, $NH_3(\tilde{A})$ correlates to $NH_2(\tilde{X}^2B_1) + H(^2S)$. For nonplanar dissociation, on the other hand, $NH_3(\tilde{A})$ decomposes to $NH_2(\tilde{A}^2A_1) + H(^2S)$ on an adiabatic potential.

Back and Koda[3] have studied the photolysis of $NH_3$ at 185.0, 206.2, and 213.9 nm, reporting that the kinetic energies of ejected H atom decrease with photolysis energies, and that internal motion of $NH_2$ is excited. Donnelly et al.[4] photolyzed $NH_3$ at 193 nm, and recorded laser-induced fluorescence (LIF) excitation spectra of the $\tilde{A}^2A_1-\tilde{X}^2B_1$ system of $NH_2$. They, however, failed to assign the spectra, which were observed immediately following photolysis, to the transitions from relatively low vibrational and rotational levels, concluding that rotational and vibrational motions of $NH_2$ fragment are highly excited. Nadtochenko et al.[37] have reported that $75 \pm 10\%$ of $NH_2$ produced in photolysis with a Xe lamp are formed in vibrationally excited states. Koplitz et al.[16] measured kinetic energy release by velocity-aligned Doppler spectroscopy of H atoms produced in the photolysis of $NH_3$ at 193 nm. They have found that the average kinetic energy of the products is about 4500 cm$^{-1}$, which corresponds to only 28% of the available energy. These facts indicate that a large amount of energy is deposited into the internal (rotational or vibrational) motion of $NH_2$. However, energy distributions were not revealed because of poor energy resolution.

In their intensive studies, the group of Ashfold and Dixon[19,23,24,29,32,33] excited $NH_3$ to single (ro)vibronic level ($v_2' = 0$ and 1) of $\tilde{A}$ state, and recorded total kinetic energy spectra by the technique of H Rydberg atom photofragment translational spectroscopy. They have found that most of the $NH_2(\tilde{X}^2B_1)$ products rotate about the *a*-axis, and rotational levels with $N \approx K_a$ are predominantly populated. The exclusive *a*-axis rotation is due to a torque made by ejected H atoms from the molecular plane of $NH_3$. It has also been found that the rotational motion of $NH_2$ is highly excited by single quantum excitation of out-of-plane vibration $v_2' = 1$ of $NH_3(\tilde{A})$. The enhancement of rotational excitation is elucidated by Coriolis coupling between $\nu_2$ ($a_2''$) and $\nu_3$ or $\nu_4$ ($e'$) vibration induced by rotation ($e''$) about the in-plane ($x,y$) internal axis of excited $NH_3(\tilde{A})$. They also excited $NH_3$ to higher vibrational levels up to $v_2' = 6$, finding that electronically excited $NH_2(\tilde{A}^2A_1)$ is produced in excitation to the parent vibrational levels $v_2' \geq 3$, and that the yield of $NH_2(\tilde{A}^2A_1)$ increases with the energies of initially prepared vibrational levels of $NH_3(\tilde{A})$. They have observed spectra indicating production of vibrationally excited $NH_2(\tilde{X}^2B_1)$; however, details about vibrational state populations have not been derived, because a given translational energy does not derive both vibrational and rotational energies of $NH_2$ fragments.

* Corresponding author. Fax: +81-25-262-7530. E-mail: yam@scux.sc.niigata-u.ac.jp

† Kobe City College of Technology.

10.1021/jp025927v CCC: $22.00 
Published on Web 07/31/2002

As described above, the UV photolysis of $NH_3$ has been extensively studied using various techniques, and textbook examples have been acquired. However, there have been few reports on the nascent vibrational energy distributions of the product $NH_2(\tilde{X}^2B_1)$. In general, highly sensitive laser-based techniques such as laser-induced fluorescence and multiphoton ionization are employed to detect product molecules, and rovibronic spectra are recorded immediately after photolysis under collision-free conditions. To determine vibrational distributions, observed signal intensities must be converted to concentrations using the detectivity of each level. The correction requires various photochemical parameters related to the observed transitions. Franck−Condon factors and Hönl−London factors are necessary to derive vibrational and rotational distributions, respectively. While there have been many reports on these factors for diatomic molecules, few accurate values for polyatomic molecules are available. The spectroscopic method described above has additional disadvantages due to some properties characteristic of $NH_2$. First, the energy differences of $K_a$ sublevels of both electronic states $\tilde{X}^2B_1$ and $\tilde{A}^2A_1$ are very large because of large $A_v - (B_v + C_v)/2$,[38−43] where $A_v$, $B_v$, and $C_v$ are rotational constants of a vibrational level $v$. Thus, the separation of subbands in $K$ structure is extraordinarily large, and a single vibronic band appears over a wide wavelength range (ca. 20 nm). The fact leads to serious congestion of transition lines and, as a consequence, assignment of observed peaks is difficult. Second, the equilibrium angle of HNH is strongly dependent on $K_a$, because $NH_2$ is a semirigid bender.[44] Consequently, Franck−Condon factors depend on both vibrational quantum number and $K_a$.[29,45] Furthermore, $\tilde{A}^2A_1$ state is perturbed by highly excited vibrational levels of $\tilde{X}^2B_1$ state, and it is very difficult to estimate accurate rotational line strength.[45,46]

In the present study, we have applied a kinetic method to determine the nascent vibrational state populations of $NH_2(\tilde{X}^2B_1, v_2'' = 0-4)$ generated in the 193 nm photolysis of $NH_3$ at 298 ± 1 K. In contrast to the conventional spectroscopic method described above, the present method needs rate constants for vibrational relaxation instead of photochemical parameters. In the actual experiment, the vibrational levels were detected first by LIF technique, and time-dependent profiles of the LIF intensities were recorded under multiple collision conditions in a buffer gas (He). Then, the rate constants for vibrational relaxation of $NH_2(\tilde{X}^2B_1, v_2'' = 1-4)$ by He were determined. Relative detectivities of the levels were derived by the kinetic analysis, which will be described in a later section, and the nascent vibrational populations of $NH_2(\tilde{X}^2B_1)$ have been obtained. We have also observed intermode coupling between the symmetric stretching ($v_1 = 1$) and bending ($v_2 = 2$) vibrations of $NH_2(\tilde{X}^2B_1)$, and we have given the rate constants for both processes ($v_1 = 1 \rightarrow v_2 = 2$ and $v_1 = 1 \leftarrow v_2 = 2$) based on the principle of detailed balance.

## Experimental Section

Experimental apparatus has been described previously,[47] and significant features of the present study are given here. $NH_3$ was photolyzed at 193 nm with an ArF excimer laser (Lambda Physik LEXtra50, 19 Hz), and $NH_2$ was generated. Vibrational levels of $NH_2(\tilde{X}^2B_1, v_2'' = 0-4$, and $v_1'' = 1)$ were detected by LIF technique. The $NH_2$ was excited via the $\tilde{A}^2A_1 - \tilde{X}^2B_1$ system with a $Nd^{3+}$:YAG laser (Spectron SL803) pumped dye laser (Lambda Physik LPD3002 with DCM), and fluorescence was collected with a lens ($f = 80$ mm) and focused on the entrance slit of a monochromator (JEOL JSG-125S, $f = 125$ cm, $\Delta\lambda$(fwhm) = 3 nm). Dispersion of the fluorescence was necessary for state selective detection, because sublevels of $K$ structure for different vibrational bands overlap one another, e.g., the ${}^rR_{0,N}$ and ${}^rQ_{0,N}$ branches of the $2_2^5$ band appear over the same wavelengths as the ${}^pR_{1,N-1}$ and ${}^pQ_{1,N}$ branches of the $2_4^7$ band, as shown in Figure 1. Excited and observed vibrational bands and their wavelengths used in the present study are listed in Table 1. The $\Delta v = 3$ sequence of vibrational bands makes it possible to excite six vibrational levels of interest with a single laser dye (DCM). Dispersed fluorescence was detected with a photomultiplier (Hamamatsu R-928). The signals from the PMT were amplified (× 10) and averaged with a gated integrator (Stanford Research SR-250), and stored on the disk of a PC through an A/D converter (Stanford Research SR-245).

The approximate concentration of $NH_2$ initially prepared can be estimated to be $\approx 3 \times 10^{12}$ cm$^{-3}$ from the energy density of the photolysis laser at the entrance window of the reaction cell (1 mJ cm$^{-2}$), photoabsorption cross section of $NH_3$: $\sigma$(193 nm) $= 1.12 \times 10^{-17}$ cm$^2$,[48] and a typical pressure of $NH_3$ (10 mTorr). Wolf et al.[49,50] have shown that formation of NH via multiphoton dissociation of $NH_3$ at 193 nm can be avoided using laser energy density less than 3 mJ cm$^{-2}$; thus, no significant NH should be produced in the present study.

When the time-dependent profiles of vibrational levels were recorded, the wavelength of the dye laser was tuned to a single rotational line and time delay between the photolysis and probe laser was continuously scanned with a homemade delay generator. After rotational motion is thermalized by collisions with a buffer gas, LIF intensity excited via a single rotational line is in proportion to the population in a vibrational level of interest. The number of data points in a time profile was 2000, and step sizes were 60−400 ns.

The flow rates of all the sample gases were controlled with calibrated mass flow controllers (Tylan FC-260KZ and STEC SEC-400 mark3) and mass flow sensors (KOFLOC 3810). Linear flow velocity was 1 m s$^{-1}$. Total pressure (He buffer) was monitored with a capacitance manometer (Baratron 122A). The total pressure measurement together with the mole fractions as measured by the flow controllers gave the partial pressures of the reagents. Highly pure grade $NH_3$ (Nihon-Sanso, 99.999%) and He (Nihon-Sanso, 99.9999%) were used without further purification.

It is well known that not only electronic ground state $\tilde{X}^2B_1$ but also excited state $\tilde{A}^2A_1$ is produced in the photolysis of $NH_3$ at 193 nm. Donnelly et al.[4] have obtained the production yield of $\tilde{A}^2A_1$ state to be about 2.5% from a measurement of fluorescence intensity. Biesner et al.[22] have reported that 26 ± 4% of the excess energies of $NH_3$ photolysis at 193.6 nm is deposited into the internal energy of $\tilde{A}^2A_1$ using the technique of H atom photofragment translational spectroscopy. They have suggested that the small yield by Donnelly et al. might be due to practical difficulties associated with detection of infrared fluorescence from low vibrational levels of $NH_2(\tilde{A}^2A_1)$. Unfortunately, both values have large errors, and branching ratios for the production of two electronic states have not been well established. However, the contribution of indirect formation of $\tilde{X}^2B_1$ from $\tilde{A}^2A_1$ must be evaluated if the value by Biesner et al. is correct.

## Results and Discussion

**Rate Constants for Vibrational Relaxation of $NH_2(\tilde{X}^2B_1, v_2'')$ by He.** Figure 1 shows dispersed LIF excitation spectra recorded in the present study. Rotational lines in the spectra except for those in the $2_3^6$ band were assigned using previously published spectroscopic data.[38−43] Significant features of the

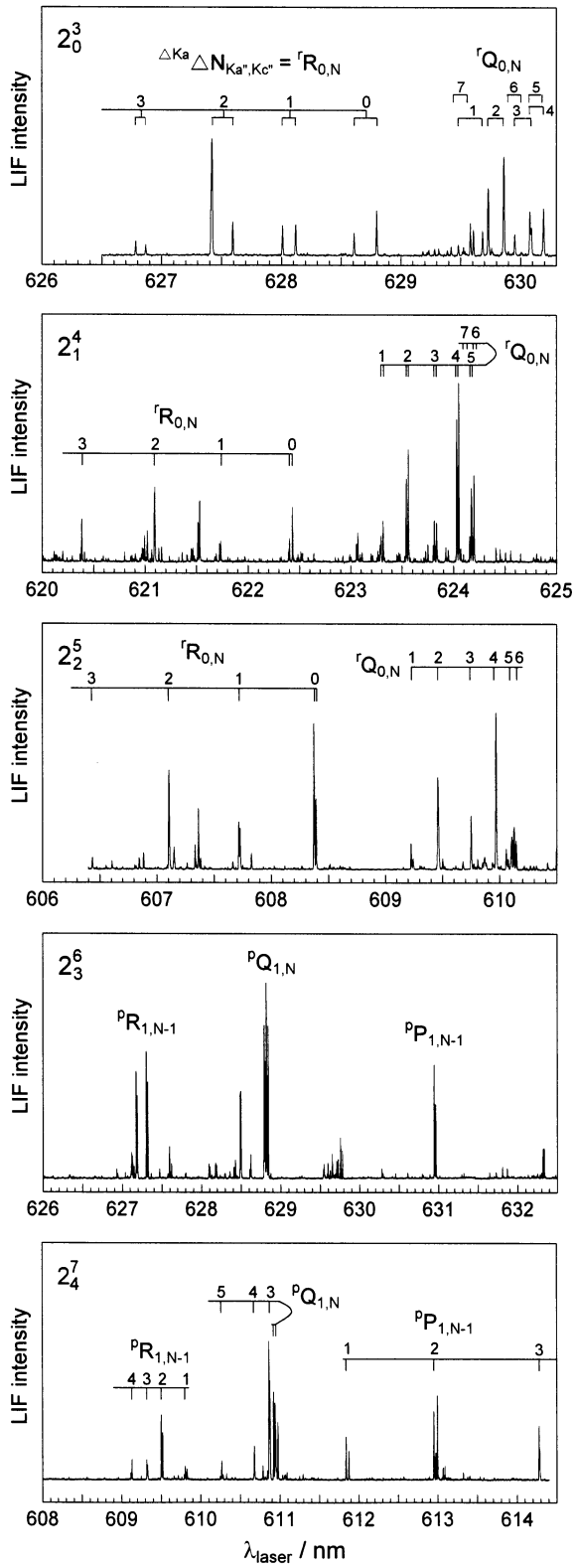


**Figure 1.** Laser-induced fluorescence (LIF) excitation spectra of $NH_2(\tilde{X}^2B_1, v_2'' = 0-4)$ excited via the $\tilde{A}^2A_1 - \tilde{X}^2B_1$ system. $P_{NH_3} =$ 10 mTorr and $P_{total}(He) = 1$ Torr. The delay times between the photolysis and probe laser were 150 $\mu$s ($2_0^3$); 75 $\mu$s ($2_1^4$); 65 $\mu$s ($2_2^5$); 40 $\mu$s ($2_3^6$); and 38 $\mu$s ($2_4^7$). Such labels as ${}^rQ_{0,N}$ are defined to be ${}^{\Delta K_a}\Delta N_{Ka,Kc}$, where $N$ is a quantum number of total angular momentum apart from spin, $K_a$ and $K_c$ are quantum numbers of the angular momenta about *a*- and *c*-axis.

branches of the $2_3^6$ band can be assigned on the analogy of the $2_4^7$ band, although there is no spectroscopic data on $v_2'' = 3$.

**TABLE 1: Excited and Observed Vibrational Bands of $NH_2$ in the $\tilde{A}^2A_1-\tilde{X}^2B_1$ System**

| excited band | $\lambda_{ex}$/nm | observed band | $\lambda_{obs}$/nm |
|---|---|---|---|
| $2_0^{3a}$ | 628 | $2_0^{3\,a}$ | 636 |
| $2_1^4$ | 623 | $2_0^4$ | 571 |
| $2_2^5$ | 610 | $2_0^5$ | 517 |
| $2_3^6$ | 629 | $2_0^6$ | 494 |
| | | $2_1^6$ | 533 |
| $2_4^7$ | 611 | $2_0^7$ | 452 |
| | | $2_1^7$ | 484 |
| $1_1^0 2_0^5$ | 620 | $2_0^5$ | 517 |

[a] Bent notation for vibrational numbering of the $\tilde{A}^2A_1$ state.

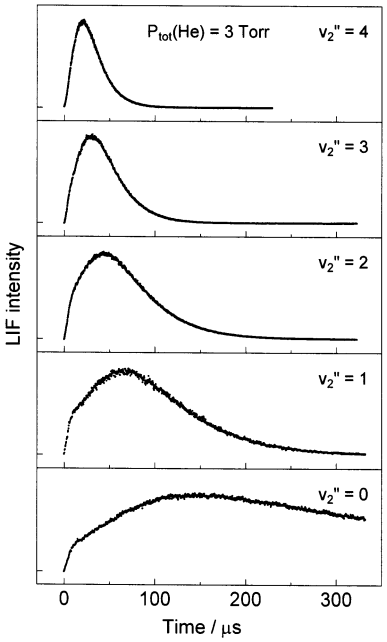


**Figure 2.** Time-dependent profiles of the LIF intensities of $NH_2(\tilde{X}^2B_1, v_2'' = 0-4)$. $P_{NH_3} = 10$ mTorr and $P_{total}(He) = 3$ Torr. The wavelengths of excitation and observation are listed in Table 1. The time axis corresponds to the delay between the photolysis and probe laser pulse. The number of time sampling points is 2000, and a single data point represents averaged signals from 10 laser pulses.

Vibrational bands of $2_0^3$ and $2_3^6$ appear over nearly identical wavelength range; nevertheless, there is no blended line in the spectra, because fluorescence from a specific vibrational level was observed. For example, fluorescence exited via the $2_0^3$ and $2_3^6$ bands was monitored at 636 nm ($2_0^3$) and 494 nm ($2_0^6$), respectively. Similarly, none of the rotational lines of the $2_2^5$ band, whose fluorescence was monitored at 517 nm ($2_0^5$), blend with those of the $2_4^7$ band monitored at 484 nm ($2_1^7$).

Figure 2 shows the time-resolved concentration profiles of $NH_2(\tilde{X}^2B_1, v_2'' = 0-4)$ recorded at 3 Torr (He) of total pressure. The time axis corresponds to the delay between the photolysis and probe laser pulse. There are 2000 points per time scan, and a single data point represents averaged signals from 10 laser pulses. Excited rotational lines are: ${}^rR_{0,2}$, ${}^rQ_{0,4}$, ${}^rQ_{0,4}$, ${}^pQ_{1,N}$ (band head), and ${}^pQ_{1,3}$ of the $2_0^3$, $2_1^4$, $2_2^5$, $2_3^6$, and $2_4^7$ bands, respectively. Five to ten profiles of a single vibrational level were recorded and averaged to obtain an adequate signal-to-noise ratio. The fast growth in the initial 10 $\mu$s, which is clearly seen in the profiles of $v_2'' = 0$ and 1, shows rotational relaxation. Approximate time constant, 6 $\mu$s, at 3 Torr gives rate constant for rotational relaxation to be $2 \times 10^{-12}$ cm$^3$ molecule$^{-1}$ s$^{-1}$. This is surprisingly small compared to normal ($\approx 10^{-10}$ cm$^3$

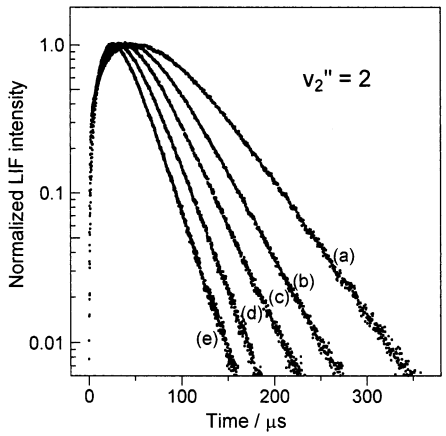


**Figure 3.** Semilogarithmic plots of the profiles of $v_2'' = 2$ at various total pressures. $P_{NH_3} = 10$ mTorr, $P_{total}(He) = 1$ Torr (a); 3 Torr (b); 5 Torr (c); 7.5 Torr (d); and 10 Torr (e). All the profiles are normalized by their maximum intensities.

molecule$^{-1}$ s$^{-1}$) rate constants for rotational relaxation. The slow rate can be elucidated by the fact that rotation about *a*-axis is exclusively excited ($N \approx K_a$) in nascent $NH_2$ fragments generated in the photolysis of $NH_3$, e.g., $K_a = 20$ in photodissociation at 216 nm.[29] Energy spacing between adjacent $K_a$ sublevels of $NH_2(\tilde{X}^2B_1)$ is so large (ca. 700 cm$^{-1}$ for $K_a \sim 20$ of $v_2'' = 0$[29]) that rotational relaxation of high $K_a$ levels is less efficient than that of low levels.

The significant growth following the rotational relaxation corresponds to vibrational relaxation from higher vibrational levels. The growth of $v_2'' = 4$ indicates that vibrational levels higher than $v_2'' = 4$ are initially generated. If the excess energy of 193 nm photolysis of $NH_3$, $h\nu$-$D_0° = 14698$ cm$^{-1}$,[33] is deposited into $\nu_2$ vibration of $NH_2(\tilde{X}^2B_1)$, levels up to $v_2'' = 10$ can be populated. The decay of $v_2'' = 0$ corresponds to a diffusion loss from the volume irradiated with a probe laser. Figure 3 shows semilogarithmic plots of observed profiles of $v_2'' = 2$ at various buffer gas pressures of He (1−10 Torr). All the profiles show growth and decay, and they may appear to fit to a biexponential expression; nevertheless, none of them can be represented by double exponential form. In the following scheme of vibrational cascade,

$$\cdots v+2 \xrightarrow{k_{v+2}} v+1 \xrightarrow{k_{v+1}} v \xrightarrow{k_v} v-1 \cdots$$

decay of a level $v$ is governed only by the apparent first-order rate constant $k_v$. On the other hand, growth is dependent not only on $k_{v+1}$ but also on $k_i$ ($i \geq v+2$). As a result, an analytical expression of the concentration profile of the level $v$ is given by the following multiple exponential form:[51]

$$[v] = \sum_{i \geq v+1} C_i e^{-k_i t} + C_v e^{-k_v t} \qquad (1)$$

The profiles shown in Figure 2 indicate that higher vibrational levels relax faster than lower levels, i.e., $k_{v+1} > k_v$. Therefore, the second term on the right side of eq 1 is predominant over other terms after a long delay time $t_1$: $C_i e^{-k_i t_1} \ll C_v e^{-k_v t_1}$. Time profiles after the time $t_1$ can be expressed by single exponential form, and semilogarithmic plots show straight lines whose slopes give the apparent first-order decay rate constants $k_v$. In the actual analysis, $t_1$ was so defined as to be a delay time after which the population of an adjacently higher vibrational level reduces to less than 3% of its maximum. For example, the delay times $t_1$ of the profiles shown in Figure 3 are 200, 155, 130, 110, and 90 $\mu$s for 1, 3, 5, 7.5, and 10 Torr of He, respectively, and profiles after $t_1$ can actually be fit to a single exponential form. Analysis by the integrated profiles method,[52−54] which has been developed by the authors, gave decay rates nearly identical to those obtained by the semilogarithmic analysis. The fact indicates that the single-exponential analysis does not underestimate decay rates by the effect of the growth due to relaxation from higher vibrational levels.

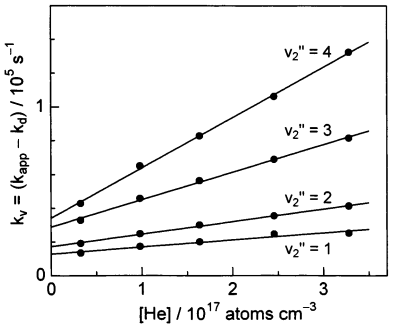


**Figure 4.** Total pressure dependence of the first-order decay rates of $NH_2(\tilde{X}^2B_1, v_2'' = 1-4)$. $P_{NH_3} = 10$ mTorr. The ordinate represents a value made by subtraction of diffusion rate from apparent decay rate at a given He pressure. The rate of diffusion at each total pressure, is determined from the decay of $v_2'' = 0$.

**TABLE 2: Rate Constants for Vibrational Relaxation of $NH_2(\tilde{X}^2B_1, v_2 = 1-4)$ by He**

| $v_2$ | $k$ (cm$^3$ molecule$^{-1}$ s$^{-1}$) | ref |
|---|---|---|
| 1 | $7 \times 10^{-14}$ | 55 |
| | $(8 \pm 0.3) \times 10^{-14}$ | 37 |
| | $(3.41 \pm 0.03) \times 10^{-13}$ | 56 |
| | $(4.2 \pm 1.0^a) \times 10^{-14}$ [b] | this work |
| 2 | $(7.5 \pm 0.5^a) \times 10^{-14}$ [b] | this work |
| 3 | $(1.6 \pm 0.1^a) \times 10^{-13}$ [b] | this work |
| 4 | $(3.0 \pm 0.1^a) \times 10^{-13}$ [b] | this work |

[a] Quoted errors are $2\sigma$. [b] Rate constant for $v_2 \rightarrow v_2-1$ relaxation.

Figure 4 shows the plots of first-order decay rates of $NH_2(\tilde{X}^2B_1, v_2'' = 1-4)$ as a function of He pressures. The ordinate represents a value made by subtraction of diffusion rate $k_d$ from apparent decay rate $k_{app}$ at each He pressure. The rate of diffusion, which depends on total pressure, is determined from the decay of $v_2'' = 0$ at a given pressure. The slopes of the plots lead to the second-order rate constants for vibrational relaxation of $NH_2(\tilde{X}^2B_1, v_2'' = 1-4)$ by collision with He: $(4.2 \pm 1.0) \times 10^{-14}$ ($v_2'' = 1$), $(7.5 \pm 0.5) \times 10^{-14}$ ($v_2'' = 2$), $(1.6 \pm 0.1) \times 10^{-13}$ ($v_2'' = 3$), $(3.0 \pm 0.1) \times 10^{-13}$ ($v_2'' = 4$) in units of cm$^3$ molecule$^{-1}$ s$^{-1}$. Quoted errors are $2\sigma$ originating in the statistical error in the single exponential analysis and the scatter of the data plotted in Figure 4. These rate constants are listed in Table 2 together with previously reported values.

While there have been three reports on the rate constants for deactivation of $v_2'' = 1$ by He, those of $v_2'' \geq 2$ are measured for the first time in the present study. The values reported by Sarkisov et al.[55] and Nadtochenko et al.[37] are about 1.8 times larger than that obtained in the present study, although their experimental conditions of sample gases ($P_{NH3} = 10$ mTorr and $P_{N2}$(buffer) = 1−5 Torr) were similar to those of our study. They determined rate constants from the growth rate of $v_2'' = 0$ instead of decay of $v_2'' = 1$. This might be a cause of their large rate constant, because growth contains a fast component due to rotational relaxation. In addition, their time sampling points were too sparse (3−7 points) to obtain accurate rate constants. Xiang et al.[56] generated vibrationally excited $NH_2$ by infrared multiphoton dissociation (IRMPD) of $CH_3NH_2$,

reporting an about 8 times larger rate constant than ours. They reported that no evidence of generation of vibrationally excited $NH_2$ was found. This is inconsistent with their previous study[57] in which they photolyzed $CH_3NH_2$ under nearly identical experimental conditions to produce vibrationally excited $NH_2$ ($v_2'' > 1$), and simulated the kinetics of vibrational relaxation on the assumption that $\nu_2$ vibration was excited up to $v_2'' = 3$. In addition, the precursor $CH_3NH_2$ has a large cross section for vibrational relaxation of $NH_2$ $(8.43 \pm 0.53) \times 10^{-11}$ cm$^3$ molecule$^{-1}$ s$^{-1}$ [56] and an apparent decay rate at zero He pressure in their measurement was about $8 \times 10^4$ s$^{-1}$. This is in marked contrast to the present study ($1.2 \times 10^4$ s$^{-1}$), and there might be some background processes in their experiments, although this is by no means certain.

The intercepts of the plots correspond to the relaxation rate by 10 mTorr of $NH_3$. Although the relatively large error of the intercepts does not permit a decisive conclusion, rate constant for vibrational relaxation of $v_2'' = 1$ by $NH_3$ can be estimated to be $(4 \pm 1) \times 10^{-11}$ cm$^3$ molecule$^{-1}$ s$^{-1}$. This value is consistent with the values reported so far: $1 \times 10^{-11}$,[55] $(9 \pm 0.3) \times 10^{-11}$,[37] and $(4.7 \pm 0.6) \times 10^{-11}$ cm$^3$ molecule$^{-1}$ s$^{-1}$.[57]

**Nascent Vibrational Distributions of $NH_2(\tilde{X}^2B_1)$ Photofragment.** LIF intensity is dependent not only on the population of detected vibrational level but also on various photochemical factors. Consequently, relative LIF intensities of two vibrational levels do not represent relative concentrations of the levels. Nevertheless, nascent vibrational distributions of $NH_2(\tilde{X}^2B_1, v_2'' = 1-4)$ generated in the photolysis of $NH_3$ at 193 nm can be derived by a simple kinetic method using vibrational relaxation rate constants obtained in the previous section.

First, the principle of the method is described. Two assumptions are made in the present analysis. First, multiple quantum relaxation ($\Delta v_2'' \geq 2$) can be neglected in collisions of $NH_2$ with He. Second, energy transfer between highly excited rotational levels of different vibrational levels, e.g., ($v_2'' = 0$, $K_a'' = 20$) $\rightarrow$ ($v_2'' = 1$, $K_a'' = 17$), can also be neglected. There has been no report giving evidence of such energy transfer in the $\tilde{X}^2B_1$ state. As seen in Figure 2, profiles of all the vibrational levels show growth and decay. At the time when a profile of vibrational level $v$ reaches its maximum, production rate of the level $v$ from $v + 1$ by relaxation balances with the total loss of the level $v$ by relaxation to $v - 1$ and diffusion. Thus, the following equation is satisfied:

$$k_{v+1}[v+1] = (k_v + k_d)[v]_{max} \tag{2}$$

where $k_{v+1}$ and $k_v$ are first-order rate constants for vibrational relaxation of levels $v + 1$ and $v$ by He and $NH_3$ ($k_v = k_v^{He}[He] + k_v^{NH_3}[NH_3]$), and $[v + 1]$ is the concentration of a level $v + 1$ at the time when a level $v$ reaches its maximum $[v]_{max}$. Unfortunately, we measure LIF intensity instead of concentration, and thus the following relation must be taken into account to deal with eq 2:

$$I_v = \alpha_v[v], \tag{3}$$

where $I_v$ and $\alpha_v$ represent observed LIF intensity and a proportionality constant as the detectivity for the level $v$, respectively. From eqs 2 and 3, relative detectivities between adjacent vibrational levels are given by the following equation:

$$\frac{\alpha_v}{\alpha_{v+1}} = \left(\frac{I_{v,max}}{I_{v+1}}\right)\left(\frac{k_v + k_d}{k_{v+1}}\right) \tag{4}$$

The first factor on the right side $I_{v,max}/I_{v+1}$ is obtained from observed profiles, and the second factor $(k_v + k_d)/k_{v+1}$ can be calculated from the rates determined in the previous section. Therefore, time-dependent profiles of two vibrational levels can be so plotted that their ordinates are common.

If a profile has a sharp rise corresponding to photolysis, nascent population ratios of two levels are readily obtained by the following equation:

$$\left(\frac{[v+1]}{[v]}\right)_{t=0} = \frac{\alpha_v}{\alpha_{v+1}}\left(\frac{I_{v+1}}{I_v}\right)_{t=0} \tag{5}$$

Unfortunately, the initial intensities of the profiles observed in the present study are not clear because of rotational relaxation (Figure 2). We, therefore, have applied integration method to obtain nascent vibrational distributions. As shown in Figure 2, there are few populations on the rotational levels at $t = 0$. This is consistent with the study by the group of Ashfold and Dixon.[19,22,24,29] They have found that rotational motion of $NH_2$ is highly excited, and most of the molecules rotate about the $a$-axis ($N'' \cong K_a''$). Relatively low rotational levels ($N'' \leq 10$) observed in the present study are populated by rotational relaxation followed by vibrational relaxation. The rate equation for a single rotational state of a vibrational level $v$ is given as follows:

$$\frac{d[v]}{dt} = \frac{1}{\tau_r}[v^*] + k_{v+1}[v+1] - (k_v + k_d)[v] \tag{6}$$

where $[v]$ is the concentration of an observed rotational level in a vibrational level $v$, $[v^*]$ is that of high rotational states of the level $v$ directly generated in the photolysis, and $\tau_r$ is an effective time constant for rotational relaxation. Here, rotational energy transfer between the observed level and a set of other rotational levels is assumed to be governed by a single rate constant $\tau_r^{-1}$.

As can be seen in time profiles shown in Figure 2, particularly $v' = 0$ and 1, the approximate time constant of rotational relaxation, $\tau_r \approx 6$ $\mu$s at 3 Torr, is shorter than those of vibrational relaxation and diffusion ($\{k_v[He]\}^{-1} \approx 35$ $\mu$s ($v_2'' = 4$) $-$ 250 $\mu$s ($v_2'' = 0$) and $k_d \approx 550$ $\mu$s), i.e., $\tau_r^{-1} \gg k_v[He]$, $k_d$. Consequently, $[v^*]$ can be expressed in the following form:

$$[v^*] = [v^*]_0 \exp(-t/\tau_r) \tag{7}$$

Substitution of $[v^*]$ in eq 6 with eq 7 followed by integration from $t = 0$ to $\infty$ gives

$$[v^*]_0 = (k_v + k_d)\int_0^\infty [v]dt - k_{v+1}\int_0^\infty [v+1]dt \tag{8}$$

because $[v]_0 = [v]_\infty = 0$. This equation indicates that nascent population of a level $v$ is given by the areas made by the profiles of the adjacent levels $v$ and $v + 1$.

The values of eq 8 for $v_2'' = 1-4$ at different total pressures (1, 3, 5, 7.5, and 10 Torr) were calculated, and relative population ratios of $v_2'' = 1-4$ have been obtained to be 1.0/1.1 $\pm$ 0.2/0.66 $\pm$ 0.3/$<$ 3.0 for $v_2'' = 1/2/3/4$. Quoted errors are $2\sigma$, and they originate in the discrepancy in the values at different total pressures. It should be noted that the population of $v_2'' = 4$ is an upper limit, because $v_2'' = 5$, which is not observed in the present study, certainly relaxes to $v_2'' = 4$, and the negative term in eq 8 corresponding to relaxation from $v_2'' = 5$ to $v_2'' = 4$ is neglected in the calculation for $v_2'' = 4$. Furthermore, the population of $v_2'' = 0$ cannot be determined by the present integration method, because vibrational levels

other than $v_2'' = 1$, e.g. $v_{1,3}'' = 1$, might relax to $v_2'' = 0$, and its contribution cannot be estimated. Fortunately, termination of rotational relaxation can be seen in the profiles of $v_2'' = 0$ and 1 (see Figure 2), and thus eq 5 can be applied for determining the ratio $([v = 0]/[v = 1])_{t=0}$. The analysis gives relative population of $v_2'' = 0/v_2'' = 1$ to be $2.2 \pm 0.7/1.0$. As a result, nascent vibrational distributions of $NH_2(\tilde{X}^2B_1)$ are obtained to be $2.2 \pm 0.7/1.0/1.1 \pm 0.2/0.66 \pm 0.3/<3.0$ for $v_2'' = 0/1/2/3/4$ (normalized by the population of $v_2'' = 1$).

The analysis described above deals with only bending vibrational mode ($\nu_2$), and no care about stretching vibrations ($\nu_1$ and $\nu_3$) has been given. The vibrational energies of the first excited levels of symmetric and asymmetric stretching modes are 3219 $cm^{-1}$ ($\nu_1$) and 3301 $cm^{-1}$ ($\nu_3$), respectively.[58] These are relatively close to the energy of $v_2'' = 2$ (2961 $cm^{-1}$). If intramolecular vibrational coupling between $v_2'' = 2$ and $v_1'' = 1$ and/or $v_3'' = 1$ is not negligible, the nascent population of $v_2'' = 2$ is likely to be overestimated. This is the case, and it is difficult to estimate the contribution of the initial populations of $v_{1,3}'' = 1$ to that of $v_2'' = 2$, determined above, because an apparent population of $v_2'' = 2$ is dependent on the initially prepared $v_{1,3}'' = 1$ and the rate constants for intra- and intermode relaxation of $\nu_1$ and $\nu_3$ vibrations.

Biesner et al.,[22] have reported that $26 \pm 4\%$ of $NH_2$ fragments generated in the photolysis at 193.6 nm are the electronically excited state $\tilde{A}^2A_1$. Loomis et al.[35] photolyzed $NH_3$ at 193 nm in the room-temperature conditions and revealed nascent vibrational energy partitioning $[v_2' = 0]:[v_2' = 1]$ of $\tilde{A}^2A_1$ state to be 3:1 by time-resolved Fourier transform infrared emission spectroscopy. The effect of indirect formation of $\tilde{X}^2B_1$ from $\tilde{A}^2A_1$ on the nascent vibrational state distributions derived in the present study must be evaluated. If deactivation from $\tilde{A}^2A_1$ to $\tilde{X}^2B_1$ is due mainly to radiative transition, population ratios of vibrational levels generated from $\tilde{A}^2A_1$ can be estimated based on the relative transition moments calculated by Jungen.[45] However, it should be noted that $NH_2(\tilde{A}^2A_1)$ is efficiently quenched even by rare gases.[59−63] Unfortunately, there is no report on the rate constants for electronic quenching of $v_2' = 0$ and 1 of $\tilde{A}^2A_1$ by He. Several groups have measured quenching rate constants of $v_2' = 3$ and 4 by collisions of He. Halpern et al.[59] measured quenching rate constant of $K_a' = 0$ of $v_2' = 4$ to be $1.45 \times 10^{-10}$ $cm^3$ $molecule^{-1}$ $s^{-1}$, Dearden et al.[62] reported $2.5 \times 10^{-11}$ $cm^3$ $molecule^{-1}$ $s^{-1}$ for $K_a' = 0$ and 2 of $v_2' = 3$ and 4, and Wysong et al.[63] gave $(2.2-5.2) \times 10^{-11}$ $cm^3$ $molecule^{-1}$ $s^{-1}$ for $K_a' = 0$ and 1 of $v_2' = 3$ and $(2.4-7.0) \times 10^{-11}$ $cm^3$ $molecule^{-1}$ $s^{-1}$ for $K_a' = 0$ and 1 of $v_2' = 4$. Dearden et al.[62] suggested that the large value by Halpern et al. might include some contribution from rotational energy transfer. Using averaged rate constants of refs 62 and 63, $4.6 \times 10^{-11}$ $cm^3$ $molecule^{-1}$ $s^{-1}$, time constants for quenching of $\tilde{A}^2A_1$ under the present experimental conditions (1−10 Torr of He) can be estimated to be 680−68 ns which are mush shorter than reported radiative lifetimes: 31.3 $\mu$s for $K_a' = 6$ of $v_2' = 0$ and 25.7−36 $\mu$s for $K_a' = 4$ and 5 of $v_2' = 1$.[61] Therefore, quenching by He is a dominant deactivation process of $\tilde{A}^2A_1$ in the present experiments. However, He is unlikely to accept about 10000 $cm^{-1}$ of excitation energy of $\tilde{A}^2A_1$. Dearden et al.[62] and Wysong et al.[63] have concluded that the surprisingly large quenching rate constants of $\tilde{A}^2A_1$ by He indicate that $NH_2(\tilde{A}^2A_1)$ transfers to nearly isoenergetic levels in $\tilde{X}^2B_1$, e.g., $v_2'' = 8$ for $v_2' = 0$ ($\Delta E = 180$ $cm^{-1}$) and $v_2'' = 9$ for $v_2' = 1$ ($\Delta E = 103$ $cm^{-1}$). Consequently, quenching of $\tilde{A}^2A_1$ by He does not generate vibrational levels observed in the present study ($v_2'' = 0-4$). Highly excited vibrational levels of $\tilde{X}^2B_1$ transferred from $\tilde{A}^2A_1$ by He undergo vibrational cascade, and pass through the levels $v_2'' = 0-4$. The fact indicates that vibrational levels observed in the present study are equally contributed by the cascade of $NH_2$ transferred from $\tilde{A}^2A_1$ by He, and no correction is needed for the vibrational distributions derived in the present study.

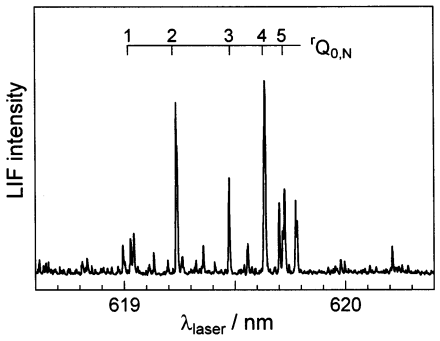


**Figure 5.** LIF excitation spectrum of $1_1^0 2_0^5$ band whose fluorescence was monitored at 517 nm ($2_0^5$). The delay time between the photolysis and probe laser was 30 $\mu$s. $P_{NH_3} = 10$ mTorr and $P_{total}(He) = 1$ Torr.

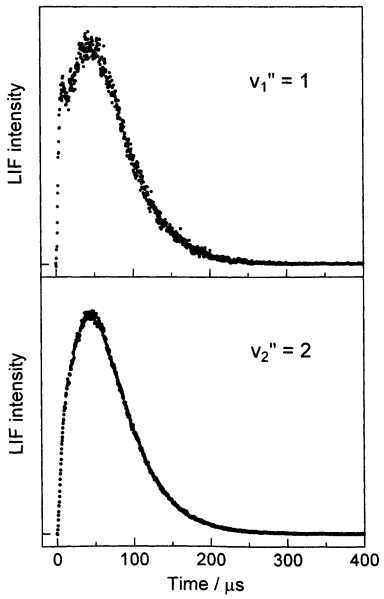


**Figure 6.** Time-dependent profiles of $v_1'' = 1$ and $v_2'' = 2$. $P_{NH_3} = 10$ mTorr and $P_{total}(He) = 3$ Torr. Two profiles are so depicted that both maximum intensities are the same. The two vibrational levels show the identical time-dependences after the initial 20 $\mu$s. The sharp peak of $v_1'' = 1$ in the early 20 $\mu$s gives evidence for fast intermode coupling between near resonant $v_1'' = 1$ and $v_2'' = 2$.

**Intermode Vibrational Coupling of $NH_2(\tilde{X}^2B_1)$.** The $v_1'' = 1$ level can be detected by LIF technique; unfortunately, there has been no report on detection of asymmetric stretching vibration ($\nu_3$) using the $\tilde{A}^2A_1 - \tilde{X}^2B_1$ transition.[58] Actually, fluorescence of the $1_{v_1}^0 2_{v_2}^v$ type combination bands were observed in dispersed fluorescence spectra; no fluorescence via the $2_{v_2}^v 3_{v_3}^0$ type bands was observed. Figure 5 shows an excitation spectrum of $1_1^0 2_0^5$ band whose fluorescence was monitored at 517 nm ($2_0^5$). The rotational lines are assigned by transition energies calculated from previously reported rotational term values.[38,64] Figure 6 shows time-dependent profiles of $NH_2(\tilde{X}^2B_1, v_1'' = 1$ and $v_2'' = 2)$ at 3 Torr of total pressure. The two vibrational levels show an identical time dependence after the initial 20 $\mu$s, indicating that the levels $v_1'' = 1$ and $v_2'' = 2$ are equilibrated by fast intermode relaxation induced by collisions with He. The findings give evidence that the nascent population of $v_2'' = 2$ obtained on the assumption of cascading

in bending vibration is overestimated. The time dependences of the profiles $v_1'' = 1$ and $v_2'' = 2$ in the initial 20 $\mu$s are totally different: $v_1'' = 1$ shows fast growth and decay, and $v_2'' = 2$ grows monotonically. The difference indicates that the initial population ratio of $v_1'' = 1$ to $v_2'' = 2$ is larger than that at equilibrium. The time scale for intermode relaxation decreased with total pressure. We have made a single-exponential analysis of the fast decay of $v_1'' = 1$ at different pressures and derived a rate constant for intermode coupling between $v_1'' = 1$ and $v_2'' = 2$ to be $[6.0 \pm 2.0(2\sigma)] \times 10^{-12}$ cm$^3$ molecule$^{-1}$ s$^{-1}$. This rate constant is a sum of the rate coefficients of forward $k_f$ ($v_2'' = 2 \rightarrow v_1'' = 1$) and backward $k_b$ ($v_2'' = 2 \leftarrow v_1'' = 1$) processes. The absolute value for each process can be derived from the sum and the ratio given by the principle of detailed balance. The relation between the forward and backward rate constants in the following process

$$NH_2(v_2 = 2) + He \underset{k_b}{\overset{k_f}{\rightleftharpoons}} NH_2(v_1'' = 1) + He \quad \Delta H = 258 \text{ cm}^{-1} \tag{9}$$

is given to be

$$\frac{k_f}{k_b} = \frac{Q_{t'}}{Q_t}\frac{Q_{r'}}{Q_r}\frac{g_{v'}}{g_v}\exp(-\Delta H/RT) \tag{10}$$

where $Q_t$ and $Q_{t'}$ are partition functions for relative translational motion of $NH_2(v_2'' = 2) + He$ and $NH_2(v_1'' = 1) + He$, $Q_r$ and $Q_{r'}$ are rotational partition functions of $NH_2(v_2'' = 2)$ and $NH_2(v_1'' = 1)$. In the present case, $Q_{t'} = Q_t$ is satisfied, because the reduced masses of $NH_2(v_2'' = 2) + He$ and $NH_2(v_1'' = 1) + He$ systems are identical, and $g_{v'} = g_v = 1$, because both $\nu_1$ and $\nu_2$ vibrations are nondegenerate. Assuming that rotational constants of $NH_2(v_2'' = 2)$ and $NH_2(v_1'' = 1)$ are the same, $Q_{r'} = Q_r$, the value of eq 10 is calculated to be $k_f/k_b = \exp(-\Delta H/RT) = 0.288$ at 298 K. This ratio ($k_f/k_b$), together with the sum $k_f + k_b$, gives the values for $k_f$ and $k_b$ to be $(1.3 \pm 0.4) \times 10^{-12}$ and $(4.7 \pm 1.6) \times 10^{-12}$ cm$^3$ molecule$^{-1}$ s$^{-1}$, respectively. The findings show that intermode vibrational relaxation between near resonant $\nu_1$ and $\nu_2$ vibrations is much faster than intramode relaxation of $\nu_2$ vibration by more than an order of magnitude. It should be noted that intermode coupling related to $v_3'' = 1$, e.g., $v_2'' = 2 \leftrightarrow v_3'' = 1$ and $v_1'' = 1 \leftrightarrow v_3'' = 1$, is not taken into account in the present scheme. Energy spacing between $v_1'' = 1$ and $v_3'' = 1$ (82 cm$^{-1}$) is much smaller than that between $v_1'' = 1$ and $v_2'' = 2$ (258 cm$^{-1}$), and consequently, vibrational coupling between $v_1'' = 1$ and $v_3'' = 1$, if any, might be faster than that between $v_1'' = 1$ and $v_2'' = 2$. Therefore, correction for the rate constants obtained in the present study must be made, if $v_3'' = 1$ is included in the coupling scheme. There has been no study of the rate constant for intermode coupling of $NH_2(\tilde{X}^2B_1)$ by He. Xiang et al.[57] have given the rate constant for $v_{1,3}'' = 1 \rightarrow v_2'' = 2$ by collisions of $CH_3NH_2$ to be $(3 \pm 1.5) \times 10^{-12}$ cm$^3$ molecule$^{-1}$ s$^{-1}$. Their value is close to ours despite a different collision partner.

The findings of the present study suggest that intermode coupling between $1_12_v$ and $2_{v+2}$ might occur for $v \geq 1$. Energy gaps between $1_12_v$ and $2_{v+2}$ increase with $v$: 325 cm$^{-1}$ for $v = 1$ and 394 cm$^{-1}$ for $v = 2$. Intermode coupling between $1_12_v$ and $2_{v+2}$ ($v \geq 1$) is expected to be less efficient than that between $1_1$ and $2_2$ (energy gap is 258 cm$^{-1}$) because relaxation rates are smaller for larger energy gap. Energy gaps between $3_12_v$ and $2_{v+2}$ also increase with $v$: 407 cm$^{-1}$ for $v = 1$ and 476 cm$^{-1}$ for $v = 2$, and coupling between $\nu_2$ and $\nu_3$ vibrations might be less efficient than that of $\nu_2$ and $\nu_1$. However, judging from only energy gaps, intermode coupling, $1_12_v$, $3_12_v \leftrightarrow 2_{v+2}$ ($v \geq 1$) is faster than intramode relaxation of $\nu_2$ vibration. We, therefore, conclude that nascent vibrational distributions determined in the present study represent population ratios between isoenergetic vibrational levels with $v_2''$, if intermode coupling among $\nu_1$, $\nu_2$, and $\nu_3$ is sufficiently faster than relaxation of $\nu_2$ vibration.

Vibrational cascade through $v_2''$ levels plays a role of "gateway" of vibrational energy relaxation of $NH_2(\tilde{X}^2B_1)$ by collisions of He, as long as intermode coupling is faster than that of intramode relaxation of $v_2''$ levels. This is the case for the present study, and measured deactivation rate constants of $v_2''$ levels by He are not affected by intermode coupling. To clarify the detailed mechanism of intermode coupling of high vibrational levels, excitation of single vibrational levels followed by probing time profiles of various vibrational levels must be realized.

## Summary

This paper describes rate coefficients for vibrational relaxation of $NH_2(\tilde{X}^2B_1)$ by collisions of He and the first detailed results on vibrational energy disposition in the $NH_2(\tilde{X}^2B_1, v_2'' = 0-4)$ fragment generated in the photolysis of $NH_3$ at 193 nm. $NH_2(\tilde{X}^2B_1, v_2'' = 0-4$ and $v_1'' = 1)$ were detected by LIF technique, and the fluorescence was dispersed to prevent spectral congestion. Sequence with $\Delta v = 3$ enables us to detect six vibrational levels with a single DCM dye. Both intramode relaxation of $\nu_2$ vibration ($v_2'' = 1-4$) and intermode coupling between $\nu_2$ and $\nu_1$ vibrations have been investigated. Rate coefficients for $v_2'' \rightarrow v_2''-1$ by collisions of He have been determined to be $(4.2 \pm 1.0) \times 10^{-14}$, $(7.5 \pm 0.5) \times 10^{-14}$, $(1.6 \pm 0.1) \times 10^{-13}$, $(3.0 \pm 0.1) \times 10^{-13}$ in units of cm$^3$ molecule$^{-1}$ s$^{-1}$ for $v_2'' = 1$, 2, 3, and 4, respectively. Rate constants for intermode coupling by He have also been given to be $(4.7 \pm 1.6) \times 10^{-12}$ ($v_1'' = 1 \rightarrow v_2'' = 2$) and $(1.3 \pm 0.4) \times 10^{-12}$ cm$^3$ molecule$^{-1}$ s$^{-1}$ ($v_1'' = 1 \leftarrow v_2'' = 2$). A simple kinetic analysis derives relative detectivities of vibrational levels from observed time profiles and provides useful relation between the initial population of a given vibrational level and the area made by the time profile of the levels. Resultant nascent vibrational distributions of $NH_2(\tilde{X}^2B_1, v_2'' = 0-4)$ generated in the photolysis of $NH_3$ at 193 nm are $2.2 \pm 0.7/1.0/<1.3/0.66 \pm 0.3/<3.0$ for $v_2'' = 0/1/2/3/4$ (normalized by the population of $v_2'' = 1$). The initial population of $v_2'' = 2$ includes a contribution of $v_1'' = 1$ and $v_3'' = 1$ by collision-induced intermode coupling by He.

**Acknowledgment.** This work was supported by the Grant-in-Aid for Scientific Research on Priority Areas "Free Radical Science" (Contract No. 05237106), Grant-in-Aid for Scientific Research (B) (Contract No. 08454181), and Grant-in-Aid for Scientific Research (C) (Contract No. 10640486) of the Ministry of Education, Science, Sports, and Culture, Japan.

## References and Notes

(1) Stefano, G. Di.; Lenzi, M.; Margani, A.; Xuan, C. N. *J. Chem. Phys.* **1977**, *67*, 3832.
(2) Koda, S.; Back, R. A. *Can. J. Chem.* **1976**, *55*, 1380.
(3) Back, R. A.; Koda, S. *Can. J. Chem.* **1977**, *55*, 1387.
(4) Donnelly, V. M.; Baronavski, A. P.; McDonald, J. R. *Chem. Phys.* **1979**, *43*, 271.
(5) Vaida, V.; Hess, W.; Roebber, J. L. *J. Phys. Chem.* **1984**, *88*, 3397.
(6) Ziegler, L. D.; Hudson, B. *J. Phys. Chem.* **1984**, *88*, 1110.
(7) Ziegler, L. D.; Kelly, P. B.; Hudson, B. *J. Chem. Phys.* **1984**, *81*, 6399.
(8) Ashfold, M. N. R.; Bennett, C. L.; Dixon, R. N. *Chem. Phys.* **1985**, *93*, 293.
(9) Ziegler, L. D. *J. Chem. Phys.* **1985**, *82*, 664.

(10) Ashfold, M. N. R.; Bennett, C. L.; Dixon, R. N. *Faraday Discuss. Chem. Soc.* **1986**, *82*, 163.
(11) Ziegler, L. D. *J. Chem. Phys.* **1986**, *84*, 6013.
(12) Xie, J.; Sha, G.; Zhang, X.; Zhang, C. *Chem. Phys. Lett.* **1986**, *124*, 99.
(13) Ziegler, L. D.; Roebber, J. L. *Chem. Phys. Lett.* **1987**, *136*, 377.
(14) Ziegler, L. D. *J. Chem. Phys.* **1987**, *86*, 1703.
(15) Ashfold, M. N. R.; Bennett, C. L.; Stickland, R. J. *Comments* At. *Mol. Phys.* **1987**, *19*, 181.
(16) Koplitz, B.; Xu, Z.; Wittig, C. *Chem. Phys. Lett.* **1987**, *137*, 505.
(17) Ziegler, L. D.; Chung, Y. C.; Zhang, Y. P. *J. Chem. Phys.* **1987**, *87*, 4498.
(18) Vaida, V.; McCarthy, M. I.; Engelking, P. C.; Rosmus, P.; Werner, H. J.; Botschwina, P. *J. Chem. Phys.* **1987**, *86*, 6669.
(19) Biesner, J.; Schnieder, L.; Schmeer, J.; Ahlers, G.; Xie, X.; Welge, K. H.; Ashfold, M. N. R.; Dixon, R. N. *J. Chem. Phys.* **1988**, *88*, 3607.
(20) Fuke, K.; Yamada, H.; Yoshida, Y.; Kaya, K. *J. Chem. Phys.* **1988**, *88*, 5238.
(21) Chung, Y. C.; Ziegler, L. D. *J. Chem. Phys.* **1988**, *89*, 4692.
(22) Biesner, J.; Schnieder, L.; Ahlers, G.; Xie, X.; Welge, K. H.; Ashfold, M. N. R.; Dixon, R. N. *J. Chem. Phys.* **1989**, *91*, 2901.
(23) Dixon, R. N. *Mol. Phys.* **1989**, *68*, 263.
(24) Ashfold, M. N. R.; Dixon, R. N.; Irving, S. J.; Koeppe, H.-M.; Meier, W.; Nightingale, J. R.; Schnieder, L.; Welge, K. H. *Philos. Trans. R. Soc.* A **1990**, *332*, 375.
(25) Endo, Y.; Iida, M.; Ohshima, Y. *Chem. Phys. Lett.* **1990**, *174*, 401.
(26) Ashfold, M. N. R.; Dixon, R. N. *Chem. Phys. Lett.* **1991**, *177*, 597.
(27) Nakajima, A.; Fuke, K.; Tsukamoto, K.; Yoshida, Y.; Kaya, K. *J. Phys. Chem.* **1991**, *95*, 571.
(28) Woodbridge, E. L.; Ashfold, M. N. R.; Leone, S. R. *J. Chem. Phys.* **1991**, *94*, 4195.
(29) Dixon, R. N.; Irving, S. J.; Nightingale, J. R.; Vervloet, M. *J. Chem. Soc., Faraday Trans.* **1991**, *87*, 2121.
(30) Henck, S. A.; Mason, M. A.; Yan, W.-B.; Lehmann, K. K.; Coy, S. L. *J. Chem. Phys.* **1995**, *102*, 4772.
(31) Henck, S. A.; Mason, M. A.; Yan, W.-B.; Lehmann, K. K.; Coy, S. L. *J. Chem. Phys.* **1995**, *102*, 4783.
(32) Mordaunt, D. H.; Ashfold, M. N. R.; Dixon, R. N. *J. Chem. Phys.* **1996**, *104*, 6460.
(33) Mordaunt, D. H.; Dixon, R. N.; Ashfold, M. N. R. *J. Chem. Phys.* **1996**, *104*, 6472.
(34) Mordaunt, D. H.; Ashfold, M. N. R.; Dixon, R. N. *J. Chem. Phys.* **1998**, *109*, 7659.
(35) Loomis, R. A.; Reid, J. P.; Leone, S. R. *J. Chem. Phys.* **2000**, *112*, 658.
(36) Calvert, J. G.; Pitts, J. N., Jr. *Photochemistry*; John Wiley and Sons: New York, 1966.
(37) Nadtochenko, V. A.; Sarkisov, O. M.; Frolov, M. P.; Tsanava, R. A.; Cheskis, S. G. *Kinet. Kataliz.* **1981**, *22*, 865.
(38) Dressler, K.; Ramsay, D. A. *Philos. Trans. R. Soc.* A **1959**, *251*, 553.
(39) Johns, J. W. C.; Ramsay, D. A.; Ross, S. C. *Can. J. Phys.* **1976**, *54*, 1804.
(40) Vervloet, M.; M.-Lafore, M. F.; Ramsay, D. A. *Chem. Phys. Lett.* **1978**, *57*, 5.
(41) Kawaguchi, K.; Yamada, C.; Hirota, E.; Brown, J. M.; Buttenshaw, J.; Parent, C. R.; Sears, T. *J. Mol. Spectrosc.* **1980**, *81*, 60.
(42) Burkholder, J. B.; Howard, C. J.; McKellar, A. R. W. *J. Mol. Spectrosc.* **1988**, *127*, 415.
(43) Ross, S. C.; Birss, F. W.; Vervloet, M.; Ramsay, D. A. *J. Mol. Spectrosc.* **1988**, *129*, 436.
(44) Duxbury, G.; Dixon, R. N. *Mol. Phys.* **1981**, *43*, 255.
(45) Jungen, C.; Hallin, K.-E. J.; Merer, A. J. *Mol. Phys.* **1980**, *40*, 25.
(46) Jungen, C.; Hallin, K.-E. J.; Merer, A. J. *Mol. Phys.* **1980**, *40*, 65.
(47) Yamasaki, K.; Tanaka, A.; Watanabe, A.; Yokoyama, K.; Tokue, I. *J. Phys. Chem.* **1995**, *99*, 15086.
(48) Atakan, B.; Jacobs, A.; Wahl, M.; Weller, R.; Wolfrum, J. *Chem. Phys. Lett.* **1989**, *155*, 609.
(49) Wolf, M.; Yang, D. L.; Durant, J. L. *J. Photochem. Photobiol.* A*: Chem.* **1994**, *80*, 85.
(50) Wolf, M.; Yang, D. L.; Durant, J. L. *J. Phys. Chem. A* **1997**, *101*, 6243.
(51) Benson, S. W. *The Foundation of Chemical Kinetics*; Robert E. Krieger Publishing: Malabar, Florida, 1982.
(52) Yamasaki, K.; Watanabe, A. B*ull. Chem. Soc. Jpn.* **1997**, *70*, 89.
(53) Yamasaki, K.; Watanabe, A.; Kakuda, T.; Tokue, I. *Int. J. Chem. Kinet.* **1998**, *30*, 47.
(54) Yamasaki, K.; Watanabe, A.; Kakuda, T.; Ichikawa, N.; Tokue, I. *J. Phys. Chem. A* **1999**, *103*, 451.
(55) Sarkisov, O. M.; Umanskii, S. Y.; Cheskis, S. G. *Dokl.* A*kad. Nauk* SSS*R* **1979**, *246*, 662.
(56) Xiang, T.-X.; Gericke, K.-H.; Torres, L. M.; Guillory, W. A. *Chem. Phys.* **1986**, *101*, 157.
(57) Xiang, T.-X.; Torres, L. M.; Guillory, W. A. *J. Chem. Phys.* **1985**, *83*, 1623.
(58) Jacox, M. E. *J. Phys. Chem. Ref. Data* **1988**, *17*, 269.
(59) Halpern, J. B.; Hancock, G.; Lenzi, M.; Welge, K. H. *J. Chem. Phys.* **1975**, *63*, 4808.
(60) Koda, S. B*ull. Chem. Soc. Jpn.* **1977**, *50*, 1683.
(61) Donnelly, V. M.; Baronavski, A. P.; McDonald, J. R. *Chem. Phys.* **1979**, *43*, 283.
(62) Dearden, S. J.; Dixon, R. N.; Field, D. *J. Chem. Soc., Faraday Trans. 2* **1982**, *78*, 1423.
(63) Wysong, I. J.; Jeffries, J. B.; Crosley, D. R. *J. Chem. Phys.* **1990**, *93*, 237.
(64) McKellar, A. R. W.; Vervloet, M. *J. Mol. Spectrosc.* **1990**, *142*, 319.